Supplemental Material for "Hydrodynamics of operator spreading and quasiparticle diffusion in interacting integrable systems"

Sarang Gopalakrishnan,[1] David A. Huse,[2] Vedika Khemani,[3] and Romain Vasseur[4]

[1]*Department of Physics and Astronomy, CUNY College of Staten Island,*
Staten Island, NY 10314; Physics Program and Initiative for the Theoretical Sciences,
The Graduate Center, CUNY, New York, NY 10016, USA
[2]*Physics Department, Princeton University, Princeton, New Jersey 08544, USA*
[3]*Department of Physics, Harvard University, Cambridge, MA 02138, USA*
[4]*Department of Physics, University of Massachusetts, Amherst, MA 01003, USA*
(Dated: November 19, 2018)

I. CONTINUITY EQUATIONS IN THE FFA MODEL

The densities or right and left moving quasiparticles in the FFA models can be written as

$$
\begin{aligned}
\rho_R(i) &= P_\uparrow(i,A)P_\uparrow(i,B) + P_\downarrow(i-1,B)P_\uparrow(i,A)P_\downarrow(i,B) + P_\downarrow(i,A)P_\uparrow(i,B)P_\downarrow(i+1,A), \\
\rho_L(i) &= P_\uparrow(i-1,B)P_\uparrow(i,A) + P_\downarrow(i-1,B)P_\uparrow(i,A)P_\downarrow(i,B) + P_\downarrow(i,A)P_\uparrow(i,B)P_\downarrow(i+1,A),
\end{aligned}
\tag{1}
$$

where $N_R = \sum_i \rho_R(i)$ and $N_L = \sum_i \rho_L(i)$ are conserved by the time evolution. It is convenient to define

$$
\begin{aligned}
\rho_+(i) &= P_\uparrow(i,A)P_\uparrow(i,B) + P_\uparrow(i-1,B)P_\uparrow(i,A) + 2P_\downarrow(i-1,B)P_\uparrow(i,A)P_\downarrow(i,B) \\
&\quad + P_\downarrow(i,A)P_\uparrow(i,B)P_\downarrow(i+1,A) + P_\downarrow(i-1,A)P_\uparrow(i-1,B)P_\downarrow(i,A), \\
\rho_-(i) &= P_\uparrow(i,A)P_\uparrow(i,B) - P_\uparrow(i,B)P_\uparrow(i+1,A).
\end{aligned}
\tag{2}
$$

The sum of these densities is also conserved, and upon coarse graining, we have $\rho_\pm(x) = \rho_R(x) \pm \rho_L(x)$. Given the simple dynamics of the FFA model, one can readily compute the time evolution of these operators over a single Floquet cycle. For example, $U^\dagger(P_\uparrow(i,A)P_\uparrow(i,B))U = P_\downarrow(i-1,B)P_\uparrow(i,A)P_\downarrow(i,B) + P_\uparrow(i-1,B)P_\uparrow(i,A)P_\downarrow(i,B)$, and $U^\dagger(P_\downarrow(i-1,B)P_\uparrow(i,A)P_\downarrow(i,B))U = P_\uparrow(i-1,B)P_\downarrow(i,A)P_\uparrow(i,B)$. Using these relations and rewriting $\rho_\pm(i,t+1) - \rho_\pm(i,t)$ as telescopic sums, we find, after a lengthy but straightforward calculation

$$
\begin{aligned}
\rho_+(i,t+1) - \rho_+(i,t) + j_+(i+1,t) - j_+(i,t) &= 0, \\
\rho_-(i,t+1) - \rho_-(i,t) + j_-(i+1,t) - j_-(i,t) &= 0.
\end{aligned}
\tag{3}
$$

The lattice currents are given by

$$
\begin{aligned}
j_+(i) &= \rho_-(i-1), \\
j_-(i) &= P_\downarrow(i-1,B)P_\uparrow(i,A)P_\downarrow(i,B) + P_\uparrow(i-1,B)P_\downarrow(i,A) + P_\downarrow(i-1,B)P_\downarrow(i,A)P_\uparrow(i,B).
\end{aligned}
\tag{4}
$$

The first equation indicates that the total current $J_+ = \sum_i j_+(i)$ is a conserved quantity, implying ballistic transport for ρ_+.

II. THERMODYNAMICS AND HYDRODYNAMICS OF THE FFA MODEL

Equilibrium states in the FFA model can be characterized by the classical partition function

$$
Z = \sum_{\{\sigma\}} e^{-\mu_R N_R - \mu_L N_L},
\tag{5}
$$

which can be computed using the 4×4 transfer matrix

$$
T = \begin{bmatrix}
1 & 1 & e^{-\mu_R - \mu_L} & e^{-\mu_R/2} \\
e^{-\mu_R - \mu_L} & e^{-\mu_R - \mu_L} & e^{-\mu_L} & e^{-\mu_R/2 - \mu_L} \\
1 & 1 & e^{-\mu_R - \mu_L} & e^{-\mu_R/2} \\
e^{-\mu_R/2} & e^{-\mu_R/2} & e^{-\mu_R/2 - \mu_L} & e^{-\mu_R - \mu_L}
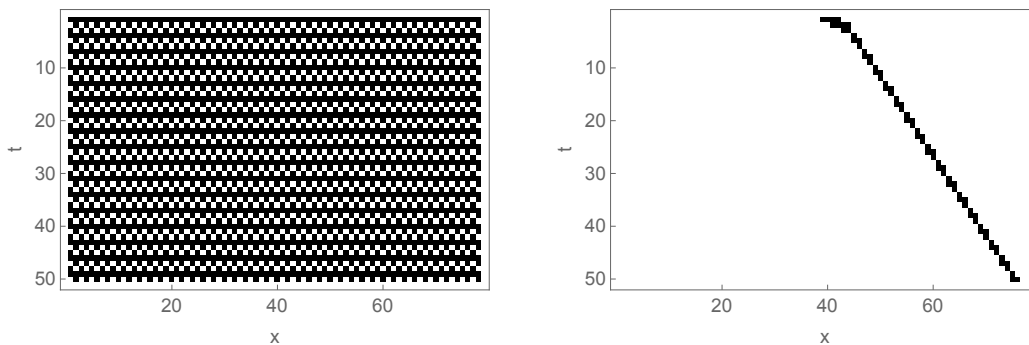\end{bmatrix},
\tag{6}
$$

FIG. 1: Nature of fluctuations and transport in the FFA model near full filling. The dynamics of the model is oscillatory with period 3 (left); thus, quasiparticles move with a velocity that also oscillates with period 3 (right). After coarse-graining in time, though, the quasiparticles can be seen to move exactly ballistically with no front-broadening.

written in the basis $\{\downarrow\downarrow, \uparrow\downarrow, \downarrow\uparrow, \uparrow\uparrow\}$. Density averages and fluctuations in the thermodynamic limit can be obtained from various derivatives of the largest eigenvalue of T. We find that the density fluctuations are non-diagonal, $\langle\delta\rho_R\delta\rho_L\rangle \neq 0$ in the right and left moving basis. However, if define the generalized "Fermi factor" $n_{R/L} = 3\rho_{R/L}/(1 + \rho_R + \rho_L)$, we find that

$$\langle(\delta n_L)^2\rangle = \langle(\delta n_R)^2\rangle = \frac{9\rho(1-\rho)}{(1+2\rho)^4\ell},$$
$$\langle\delta n_R\delta n_L\rangle = 0, \tag{7}$$

for a system of size ℓ in an equilibrium state with filling $\rho = \rho_R = \rho_L$.

Using this transfer matrix, we can also compute the equilibrium averages of the currents $j_\pm = \rho_R v_R \pm \rho_L v_L$. We find

$$v_{R/L} = \pm 1 \mp \frac{2\rho_{L/R}}{1 + \rho_R + \rho_L}. \tag{8}$$

This formula coincides with the velocities of a hard rod gas with only two "bare" velocities $v_R^0 = 1$ and $v_L^0 = -1$, and effective length $a = -1$.[1,2] One can also understand this formula in an elementary way as follows: if a right mover starts at $(0,0)$ and goes to (x,t), it encounters all the left movers that started at points closer than $x - v_L t$. The time t is determined by accounting for the fact that the "bare" velocity is 1, and that each collision with a left mover adds an extra time step. This means that $t = x + \rho_L(x - v_L t)$, which yields $v_R = x/t = (1 + \rho_L v_L)/(1 + \rho_L)$. Repeating the argument for left movers, we find $v_L = (-1 + \rho_R v_R)/(1 + \rho_R)$. Solving these two equations yields (8). Note that this formula is consistent with

$$j_+ = \rho_R - \rho_L, \tag{9}$$

as it should since this relation holds exactly microscopically.

Since the microscopic averages of the currents coincide with this hydrodynamic expectation, one might be tempted to use the variance of the microscopic current instead of the expression we obtained from the density fluctuations and the coarse-grained velocity formulas (8). These two expressions do *not* agree; the discrepancy between them can be seen, and its mechanism most clearly understood, near the fully filled limit. At full filling, the dynamics consists of persistent period-3 oscillations (Fig. 1); the current oscillates in a 100100100 ... sequence. These current fluctuations, though strong, are not *random*, and they cause deterministic rather than random changes of the front velocity. After time averaging, these fluctuations cancel out exactly except for boundary terms. Thus they are not responsible for diffusive broadening. Instead, the fluctuations that cause diffusive broadening are the slow, random fluctuations that survive under coarse-graining.

The Euler hydrodynamics in the quasiparticle language (corresponding to the kinetic theory of these quasiparticles), leads to the following continuity equations

$$\partial_t \rho_{R/L} + \partial_x(v_{R/L}[\rho_R, \rho_L]\rho_{R/L}) = 0. \tag{10}$$

Using the definition of the "Fermi factors" above, we find the advection equations

$$\partial_t n_{R/L} + v_{R/L}[n_R, n_L]\partial_x n_{R/L} = 0. \tag{11}$$

This is a general property of Fermi factors in generic integrable systems.[3,4]

III.   QUASIPARTICLE DIFFUSION IN GENERIC INTEGRABLE MODELS

In this section, we derive explicitly the form of the quasiparticle diffusion using the kinetic theory argument given in the main text. The hydrodynamic equations for quantum integrable systems can be thought of either as Euler equations for all the (local and quasi-local) conserved quantities, or equivalently, as a kinetic equation for the quasiparticles. Let us define densities of *particles*, *holes* and *states* via

$$\ell\rho_k dk = \{\# \text{ occupied pseudo-momenta in } [k, k+dk)\}$$
$$\ell\rho_k^h dk = \{\# \text{ unoccupied pseudo-momenta in } [k, k+dk)\}$$
$$\ell\rho_k^{\text{tot}} dk = \{\# \text{ allowed pseudo-momenta in } [k, k+dk)\}. \tag{12}$$

respectively, for a system of size ℓ. For simplicity, we are using a shorthand notation for k which labels both the types of quasiparticles and their pseudo-momenta. Let $\rho_k^{\text{tot}} = \rho_k + \rho_k^h$ be the total density of states, and it is also useful to define the generalized Fermi factor, given by $n_k = \frac{\rho_k}{\rho_k^{\text{tot}}}$, which is by definition a number between 0 and 1. These quantities are related by the *Bethe equations*

$$\rho_k^{\text{tot}} + \int_{-\infty}^{\infty} \mathcal{K}(k, k')\rho_{k'} dk' = \frac{\partial_k p_k^0}{2\pi}, \tag{13}$$

for some scattering kernel $\mathcal{K}(k, k')$ whose precise form depends on the integrable model under consideration, with p_k^0 the bare momentum. A given generalized Gibbs ensemble (GGE) state – including thermal states in particular – can be shown to correspond to a given distribution of quasi-particles ρ_k. Note that we can also choose to work with the Fermi factor n_k, since the Bethe equation together with $\rho_k^{\text{tot}} = \rho_k + \rho_k^h$ fully fix the other distributions once n_k is known.

Assuming local equilibrium, we can imagine that these quantities all depend on x and t, and that the Bethe equation (13) is satisfied locally. The semi-classical kinetic equation for n_k is then quite simple[3,4]

$$\partial_t n_k + v_k[n]\partial_x n_k = 0, \tag{14}$$

where $v_k[n]$ is the group velocity of the quasi-particles which can also be computed from Bethe ansatz. The effective group velocity[5] is then given by $v_k[n] = \frac{\epsilon_k'[n]}{p_k'[n]}$, where ϵ_k' and p_k' are the dressed derivatives of the quasiparticle energy and momentum, given by

$$\epsilon_k' + \int dk' \mathcal{K}(k - k')n_{k'}\epsilon_{k'}' = \partial_k \epsilon_k^0, \tag{15}$$

$$p_k' + \int dk' \mathcal{K}(k - k')n_{k'}p_{k'}' = \partial_k p_k^0. \tag{16}$$

with ϵ_k^0 and p_k^0 the bare energy and momentum. Note that these equations are time-reversal invariant and ignore the density fluctuations responsible for diffusion that we now describe.

For a system of size ℓ, the fluctuations of the quasiparticle densities in a thermal state at temperature T (corresponding to an equilibrium Fermi factor n_k given by the thermodynamic Bethe ansatz)[6] read[7]

$$\langle \delta n_k \delta n_{k'} \rangle = \frac{1}{\rho_k^{\text{tot}}\ell} n_k(1 - n_k)\delta(k - k'). \tag{17}$$

As explained in the main text, these fluctuations should be computed over a distance $\ell = |v_k - v_{k'}|t$. This leads to a broadening of the quasiparticle trajectories

$$\delta x_k^2(t) = t \int dk' \left(\frac{\delta v_k}{\delta n_{k'}}\right)^2 \frac{n_{k'}(1 - n_{k'})}{\rho_{k'}^{\text{tot}} |v_k - v_{k'}|}. \tag{18}$$

The last step of the calculation is to compute the functional derivative $\frac{\delta v_k}{\delta n_{k'}}$ using eqs. (15) and (16). We see that we have $\frac{\delta \epsilon_k'}{\delta n_{k'}} = v_{k'} \frac{\delta p_k'}{\delta n_{k'}}$, so that

$$\frac{\delta v_k}{\delta n_{k'}} = \frac{v_{k'} - v_k}{p_k'} \frac{\delta p_k'}{\delta n_{k'}} = \frac{v_{k'} - v_k}{\rho_k^{\text{tot}}} \frac{\delta \rho_k^{\text{tot}}}{\delta n_{k'}}, \tag{19}$$
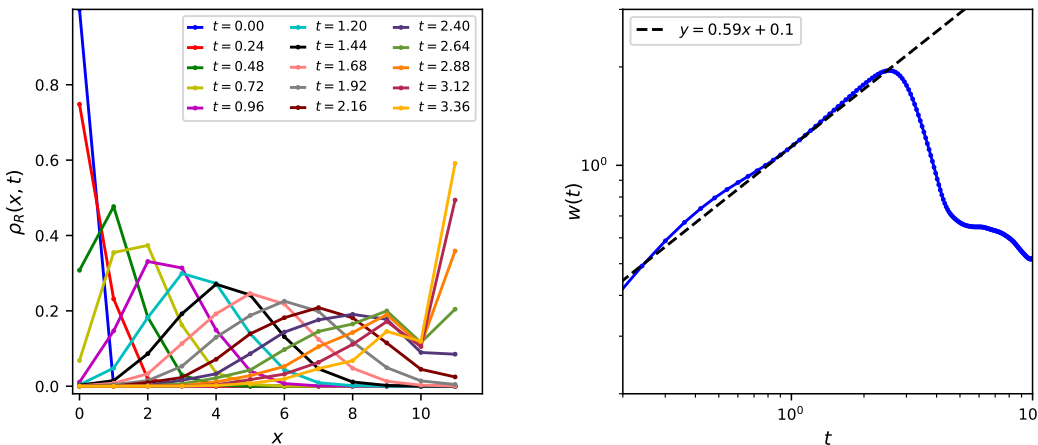
FIG. 2: (left) Right weight $\rho_R(x,t)$ for the spreading operator $\sigma_0^x(t)$ in an XXZ chain of size $L = 12$ with $\Delta = 0.5$ showing ballistic front propagation with front broadening. Width of the spreading front $w(t)$ shows a scaling consistent with $w(t) \sim t^{1/2}$ (dashed line: fit with $x = \log t$ and $y = \log w$). Note that we have very limited dynamical range in time before the front reaches the end of the chain, but the numerical exponent is already quite far from the free fermion result $w(t) \sim t^{1/3}$.

since $p'_k = 2\pi\rho_k^{\rm tot}$ (see also Refs.8,9 for related formulas). Let $-\frac{1}{p'_{k'}}\frac{\delta p'_k}{\delta n_{k'}} \equiv \mathcal{K}^{\rm dr}(k,k')$. Using (16), this "dressed kernel" satisfies the integral equation

$$\mathcal{K}^{\rm dr}(k,k') = \mathcal{K}(k,k') - \int dk'' \mathcal{K}(k,k'')\mathcal{K}^{\rm dr}(k'',k')n_{k''}. \tag{20}$$

In terms of the dressed kernel, we have $\left(\frac{\delta v_k}{\delta n_{k'}}\right)^2 = (v_k - v_{k'})^2 \left[\mathcal{K}^{\rm dr}(k,k')\right]^2 \left(\frac{\rho_{k'}^{\rm tot}}{\rho_k^{\rm tot}}\right)^2$. Plugging this expression in (18), we find

$$\delta x_k^2(t) = t\frac{1}{(\rho_k^{\rm tot})^2} \int dk' |v_k - v_{k'}| \left[\mathcal{K}^{\rm dr}(k,k')\right]^2 \rho_{k'}(1 - n_{k'}), \tag{21}$$

as claimed in the main text. This formula can be evaluated in any equilibrium (GGE) state.

IV. NUMERICS ON THE XXZ SPIN CHAIN

We now present some numerics on the XXZ chain using exact diagonalization. Despite the small sizes and times accessible to this study, we see many signatures of the qualitative features discussed in the main text, including the diffusive front broadening of operators.

The Hamiltonian is

$$H = \sum_i \sigma_i^x \sigma_{i+1}^x + \sigma_i^y \sigma_{i+1}^y + \Delta\sigma_i^z \sigma_{i+1}^z \tag{22}$$

where $\sigma_i^{x/y/z}$ are Pauli spin 1/2 operators on site i and we pick $\Delta = 0.5$ for specificity. For a spin-1/2 chain of length L, a complete orthonormal basis for all operators is given by the 4^L "Pauli strings" $\mathcal{S}$, which are products of Pauli matrices on distinct sites. We can then express our spreading operator in this basis of Pauli strings:

$$O_0(t) = \sum_\mathcal{S} a_\mathcal{S}(t)\mathcal{S}. \tag{23}$$

We measure the right front of the spreading operator $O(t)$ using the "right-weight" $\rho_R(x,t)$, defined as the total weight in $O(t)$ of basis strings that end at site x — which means that they act as the identity on all sites to the right of site x, but act as a non-identity on site x:

$$\rho_R(x,t) = \sum_{\substack{\text{strings } \mathcal{S} \text{ with} \\ \text{rightmost non-} \\ \text{identity on site } x}} |a_\mathcal{S}|^2, \qquad \sum_i \rho_R(x,t) = 1. \tag{24}$$
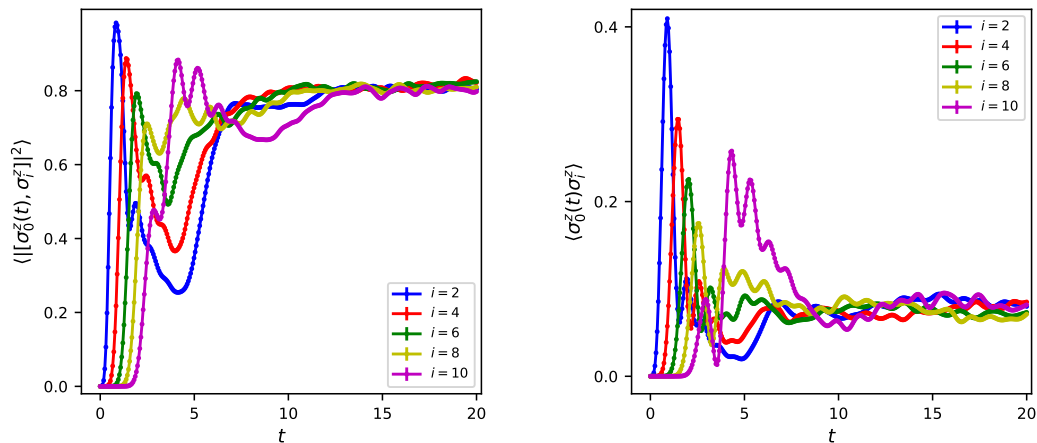
FIG. 3: (left) Two-point time-ordered correlators and OTOCs in the XXZ model at $\Delta = 0.5$ showing that both these quantities detect the operator front(s), although they saturate to different values at late times. The multiple fronts visible in the data is consistent with the presence of multiple species of quasiparticles.

The conservation law on $\rho_R(x,t)$ follows from unitarity and supports the identification of this quantity as an "emergent" density undergoing biased diffusion.[10,11] The left front can be defined analogously. Fig 2 (right) shows $\rho_R(x,t)$ for an initial operator $O_0 = \sigma_0^x$ at different times in a system of length $L = 12$. We clearly see front propagating ballistically to the right as the weight of $O(t)$ spreads to longer Pauli strings; we also clearly see the front getting broader with increasing time before it reaches the end of the chain. We can quantify the width of the front by looking at the second moment of $\rho_R(x,t)$ in time:

$$w(t) = \sqrt{\sum_x x^2 \rho_R(x,t) - \left(\sum_x x \rho_R(x,t)\right)^2}. \tag{25}$$

Fig 2 (left) shows $w(t)$ plotted against time. While we have very limited dynamical range in time before the front reaches the end of the chain (and after an initial transient), the data seems consistent with a $w(t) \sim t^{1/2}$ scaling, and certainly quite far from the free fermion result of $w(t) \sim t^{1/3}$. The data for the spreading of $\sigma_0^z(t)$ looks very similar.

Next, we look at the behavior of two-point correlators and OTOCs: $\langle \sigma_0^z(t) \sigma_i^z(t) \rangle$ and $\langle |[\sigma_0^z(t), \sigma_i^z(t)]|^2 \rangle$ in Fig 3. We see that *both* the two-point correlator and the OTOC are able to detect the operator front for integrable systems, unlike the case of non-integrable systems (although two-point functions may not always work for this purpose, for example when additional symmetries force these to be zero or subballistic). Notice that the figures show the appearance of multiple fronts which is consistent with the presence of multiple species of quasiparticles in the XXZ model, each with their own "fastest" speed. Further, as discussed in the main text, while the two point function decays at late times, the OTOC generically saturates to a non-zero value as the front fills in. The saturation value of the OTOC is approximately 0.8 which is less than the generic value of 1 in chaotic systems. However, this difference is small and the saturation does show a weak increase with increasing system size (not shown). Whether this saturation value converges to a distinct universal value in large systems is presently unclear to us, but the difference is certainly weak. We note also that the non-monotonic behavior of the OTOC before saturation is generally not seen in chaotic models, so this may again be a weak signature of the lack of chaos. But the origin and universality of this behavior is again presently unsettled.

[1] H. Spohn, *Large scale dynamics of interacting particles*, Texts and monographs in physics (Springer-Verlag, 1991).
[2] B. Doyon and H. Spohn, Journal of Statistical Mechanics: Theory and Experiment **2017**, 073210 (2017).
[3] B. Bertini, M. Collura, J. De Nardis, and M. Fagotti, Phys. Rev. Lett. **117**, 207201 (2016).
[4] O. A. Castro-Alvaredo, B. Doyon, and T. Yoshimura, Phys. Rev. X **6**, 041065 (2016).
[5] L. Bonnes, F. H. L. Essler, and A. M. Läuchli, Phys. Rev. Lett. **113**, 187203 (2014).
[6] M. Takahashi, *Thermodynamics of One-Dimensional Solvable Models* (Cambridge University Press, 1999).
[7] P. Fendley and H. Saleur, Phys. Rev. B **54**, 10845 (1996).

[8] V. B. Bulchandani, R. Vasseur, C. Karrasch, and J. E. Moore, Phys. Rev. Lett. **119**, 220604 (2017).

[9] V. B. Bulchandani, Journal of Physics A: Mathematical and Theoretical **50**, 435203 (2017).

[10] A. Nahum, S. Vijay, and J. Haah, Phys. Rev. X **8**, 021014 (2018).

[11] C. W. von Keyserlingk, T. Rakovszky, F. Pollmann, and S. L. Sondhi, Phys. Rev. X **8**, 021013 (2018).